Meteorologische Zeitschrift, Vol. **14**, No. 6, 735-745 (December 2005)

Article

The portable university model of the atmosphere (PUMA): Storm track dynamics and low-frequency variability

KLAUS FRAEDRICH*, EDILBERT KIRK, UTE LUKSCH and FRANK LUNKEIT

Meteorological Institute, University of Hamburg, Germany

(Manuscript received February 2, 2005; in revised form May 17, 2005; accepted September 28, 2005)

Abstract

The ability of analysing atmospheric dynamics by idealized experiments using a simplified circulation model is illustrated in three related studies. The investigations focus on the organization of localized strom tracks, their impact on low-frequency variability, and on the response to external thermal forcing. A localized storm track in agreement with observations is forced by a heating dipole embedded in a zonally symmetric field if the dipole orientation corresponds to the Northern Hemisphere winter case. The interaction of two storm tracks leads to low-frequency variability. Spatial resonance between a low-frequency large scale retrograde travelling wave and the storm track eddies is identified causing the fluctuations. Teleconnection pattern remarkably similar to the observed North Atlantic Oscillation (NAO) and Pacific North American (PNA) pattern emerge when the distance of the two storm tracks is set to the observed value of about 150°. While the spatial resonance mechanism forces the NAO-like pattern, baroclinic processes are related to the PNA-like teleconnection. Anomalies induced by large scale thermal forcing strongly depend on the background flow. A non-linear response is observed in the model depending on the sign of the forcing and its position relative to the storm track. A baroclinic and an equivalent barotropic component defines the response. In addition, the change of the space-time variability is affected by eddy feedbacks.

Zusammenfassung

Die Leistungsfähigkeit von idealisierten Experimenten mit einem vereinfachten Zirkulationsmodell bei der Analyse der atmosphärischen Dynamik wird anhand dreier miteinander verbundener Studien veranschaulicht. Die Untersuchungen konzentrieren sich auf die Organisation lokalisierter Stormtracks und deren Einfluss auf die niederfrequente Variabilität sowie die Antwort auf einen externen Antrieb. Ein lokalisierter Stormtrack in Übereinstimung mit Beobachtungen wird durch einen Heizungs-Dipol erzeugt, der in ein zonal symmetrisches Feld eingebettet ist und dessen Orientierung dem nordhemisphärischen Winter Fall entspricht. Die Wechselwirkung zweier Stormtracks führt zu langperiodischen Schwankungen. Ein Mechanismus räumlicher Resonanz zwischen langperiodischen, mit einer retrograd wandernden Welle verbundenen Schwankungen, und den synoptischen Störungen des Stormtracks wird als Ursache der Variabilität identifiziert. Telekonnektionsmuster, die bemerkenswert mit der Nord-Atlantischen Oszillation (NAO) und dem Pazifik Nord-Amerikanischen (PNA) Muster übereinstimmen, treten bei einem Stormtrack Abstand von 150° auf. Während die räumliche Resonanz das simulierte NAO-Muster antreibt, sind im Modell barokline Prozesse mit dem PNA-Muster verbunden. Durch einen großskaligen thermischen Antrieb verursachte Anomalien hängen vom Grundzustand ab. Eine nichtlineare Antwort abhängig vom Vorzeichen und der Position des Antriebs wird beobachtet, die sich aus einem baroklinen und einem äquivalent barotropen Anteil zusammensetzt. Auch die Variabilität in Raum und Zeit wird durch Rückkopplungsmechanismen mit den Stormtrack Störungen beeinflusst.

1 Introduction

The concentration of mid-latitude eddy activity in the so called North Atlantic and North Pacific storm track is a basic feature of the Northern Hemisphere wintertime circulation (BLACKMON, 1976; BLACKMON et al., 1977; LAU, 1979a, b). The physical mechanism for the organization, however, is less clear. In principal, the storm tracks may organize themselves by the feedback of the eddies with the time mean flow (CHANG and ORLANSKI, 1993). An alternative mechanism is the localization of eddy activity by temperature gradients maintained by the land-sea contrasts and fixed by heating and orographic forcing (SMAGORINSKY, 1953; HELD, 1983; HOSKINS and VALDES, 1990; TING, 1994).

Another feature of the Northern Hemisphere midlatitude atmospheric circulation is its low-frequency variability which to a large amount can be described by a few geographically fixed circulation regimes referred to as teleconnections like the Pacific North American Pattern (PNA) or the North Atlantic Oscillation (NAO) (WALLACE and GUTZLER, 1981). These teleconnection patterns undergo distinct life cycles with time scales of some 10 days (FELDSTEIN, 1998, 2002). The role of the storm track eddies for the observed low-frequency variability is not totally assessed so far. In addition, the

*Corresponding author: Klaus Fraedrich, Meteorologisches Institut, Universität Hamburg, Bundesstraße 55, 20146 Hamburg, e-mail: fraedrich@dkrz.de

0941-2948/2005/0074 $ 4.95

DOI: 10.1127/0941-2948/2005/0074

interaction of the two storm tracks may be a source of circulation anomalies (FRAEDRICH et al., 1993; SICKMÖLLER et al., 2000).

Large scale thermal forcing like North Atlantic sea surface temperature anomalies on interannual or interdecadal time scales can induce an atmospheric response by exiting stationary waves or altering the behavior of the transients (BJERKNES, 1964; PALMER and SUN, 1985; PENG et al., 1997). Various feedback mechanisms have been discussed (see, for example, reviews by FRANKIGNOUL, 1985 and LAU, 1997) but a full understanding is still lacking. Also in this case, the localized storm tracks may play an important role.

While observations and comprehensive models provide extensive information on many aspects of the atmospheric circulation, its variability and its response to external forcing, the use of simplified models may be a promising additional approach. Systematic idealized sensitivity experiments at low computational costs can gain deep insight into certain aspects by analysing the underlying physical mechanisms. In this respect, this paper collects three studies performed with a simplified atmospheric global circulation model aiming on (i) the organization of localized storm tracks by diabatic heating (FRISIUS et al., 1998) and their effect on (ii) low-frequency variability (FRANZKE et al., 2000, 2001) and on (iii) the atmospheric response to external thermal forcing (WALTER et al., 2001). Section 2 and Section 3 describe the model and the experimental setups, respectively. The results of the different sets of sensitivity experiments are presented in Section 4. The paper closes with a discussion and conclusions in Section 5.

2 Model

The experiments are performed using the simplified global atmospheric circulation model PUMA (Portable university model of the atmosphere; FRAEDRICH et al., 1998[1]). PUMA is a modern version of the spectral global model introduced by HOSKINS and SIMMONS (1975) and JAMES and GRAY (1986). The model solves the primitive equations on the sphere utilizing the spectral transform method (ELIASEN et al., 1970; ORSZAG, 1970) together with a semi-implicit time differencing scheme. In the vertical, equally spaced sigma levels are used. While the dry dynamics represents the core of a state-of-the-art atmospheric general circulation model (AGCM), simple and linear parameterizations for abatic heating and dissipation replace the sophisticated parameterization packages of an AGCM. Moisture is not considered explicitly. Following JAMES and GRAY (1986) and HELD and SUAREZ (1994) a Newtonian cooling formulation parameterizes the diabatic heating/cooling. The actual model temperature T is relaxed towards a prescribed three-dimensional restoration temperature field T_R within the time scale τ_R:

$$\left(\frac{\partial T}{\partial t}\right)_{\text{cooling}} = \frac{T_R - T}{\tau_R} \tag{2.1}$$

Surface friction is incorporated via a Rayleigh friction acting on divergence D and relative vorticity ξ with a time scale τ_F:

$$\left(\frac{\partial(\xi,D)}{\partial t}\right)_{\text{friction}} = -\frac{(\xi,D)}{\tau_F} \tag{2.2}$$

A hyperdiffusion ($\sim \nabla^8$) represents the effect of non-resolved eddies on the energy and enstrophy cascade:

$$\left(\frac{\partial(T,\xi,D)}{\partial t}\right)_{\text{diffusion}} = \frac{\nabla^8(T,\xi,D)}{\tau_D} \tag{2.3}$$

where τ_D gives the characteristic time scale.

3 Experimental design

All experiments are performed utilizing a PUMA version with T21 horizontal resolution (approx. 5.6° x 5.6° on the corresponding Gaussian grid) and five equally spaced sigma levels in the vertical. A time step of one hour is used. Orographic forcing is omitted. Rayleigh friction is applied to the lower most model level only and the time scale τ_F is one day. The hyperdiffusion is set to damp the smallest wave number with a time scale of 0.25 days. The time scale for the Newtonian cooling τ_R is 30 days for the upper three levels (sigma= 0.1, 0.3, 0.5), 10 days for sigma= 0.7 and 5 days for sigma= 0.9. All experiments were run for several decades where the first years are not considered for the subsequent analyses.

While all the above is common for all experiments described in this paper, the simulations differ with respect to the zonal asymmetries of the spatial distribution of the restoration temperature field T_R embedded in a zonally symmetric profile (Fig. 1). The zonally symmetric component of T_R is defined by an equator to pole temperature contrast of 70 K at the surface which decreases to zero at the tropopause (which height is set to 12 km). The mean tropospheric lapse rate of T_R is -6.5 K/km. Three sets of experiments are accomplished:

(i) The organization of variability of a single storm track

To study the organization and variability of a single storm track a temperature dipole is superimposed on the zonally symmetric temperature profile (sketched in Fig.

[1] www.mi.uni-hamburg.de3/puma

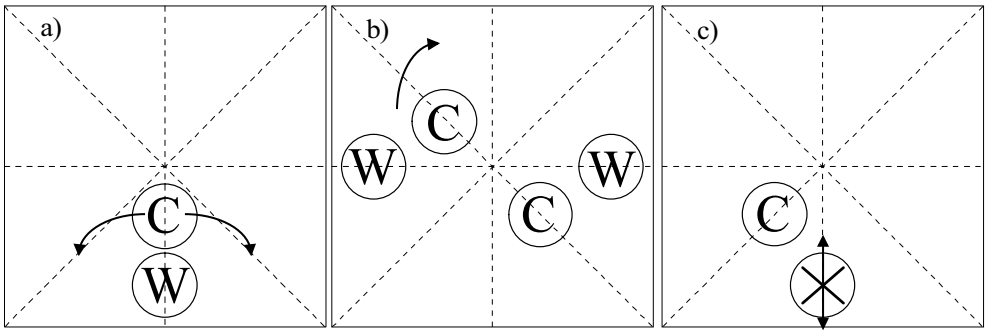

Figure 1: Sketch of the zonally asymmetric components of the reference temperature T_R. (a) Dipole orientation NE, Z or SE to force a single storm track. (b) Two NE-dipoles with different distances. (c) Monopole (cross) added to the NE-dipole varying its position. C and W denote the cold and the warm pole, respectively.

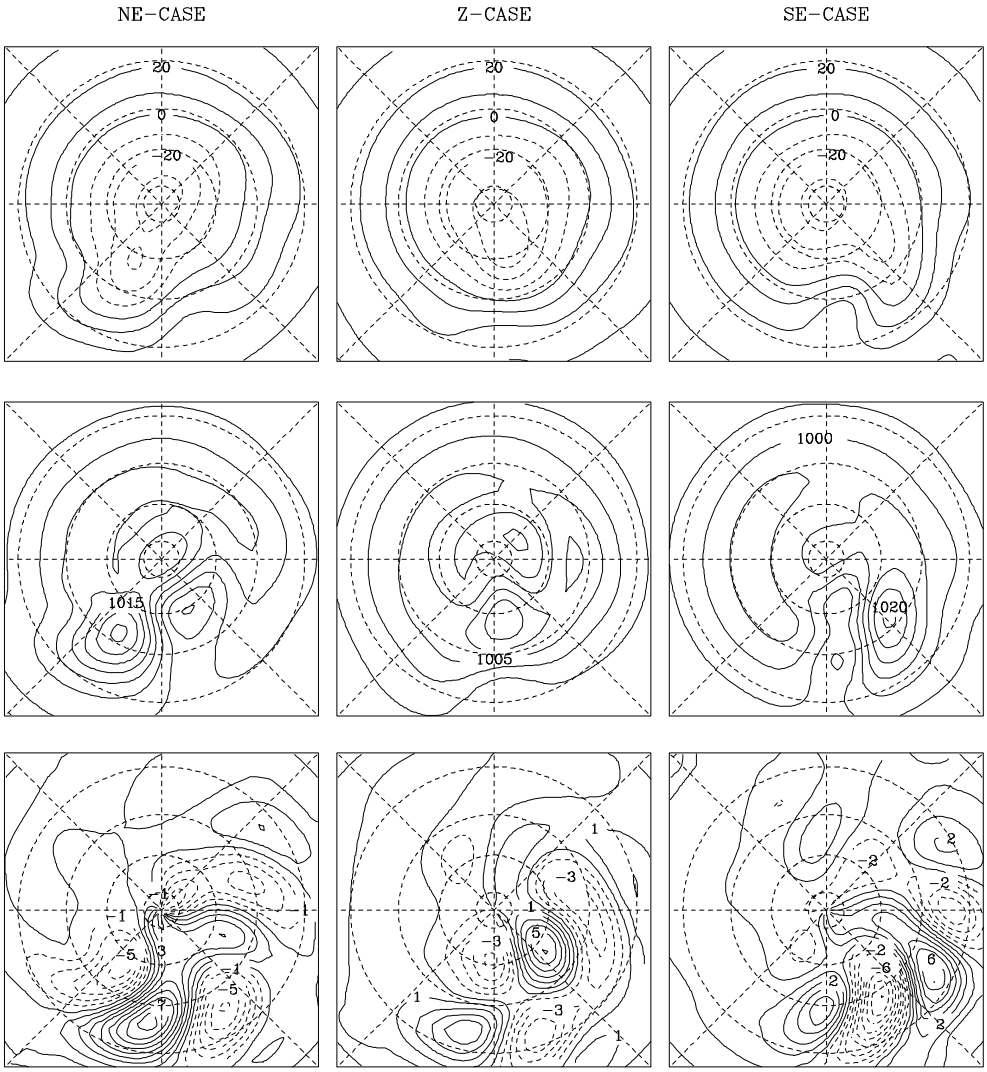

Figure 2: Climatological hemispheric distribution of the simulated temperature at 900 hPa (in °C, upper panels), surface pressure (in hPa, middle panels) and meridional wind at 300 hPa (in m/s, lower panels) for the NE-case (right column), the Z-case (middle column) and the SE-case (right column).

1a). The dipole anomalies of the restoration temperature have magnitudes of 50 K in the lowermost model level (sigma= 0.9). Due to the Newtonian cooling formulation this leads to heating anomalies of about 10 K/day. Three experiments with different orientation of the dipole are performed: The NE-case (a north-east orientation of the isolines) corresponding to a Northern Hemisphere winter, the Z-case (zonal orientation) which is more similar to a Northern Hemisphere summer and the somewhat artificial SE-case (south-east orientation).

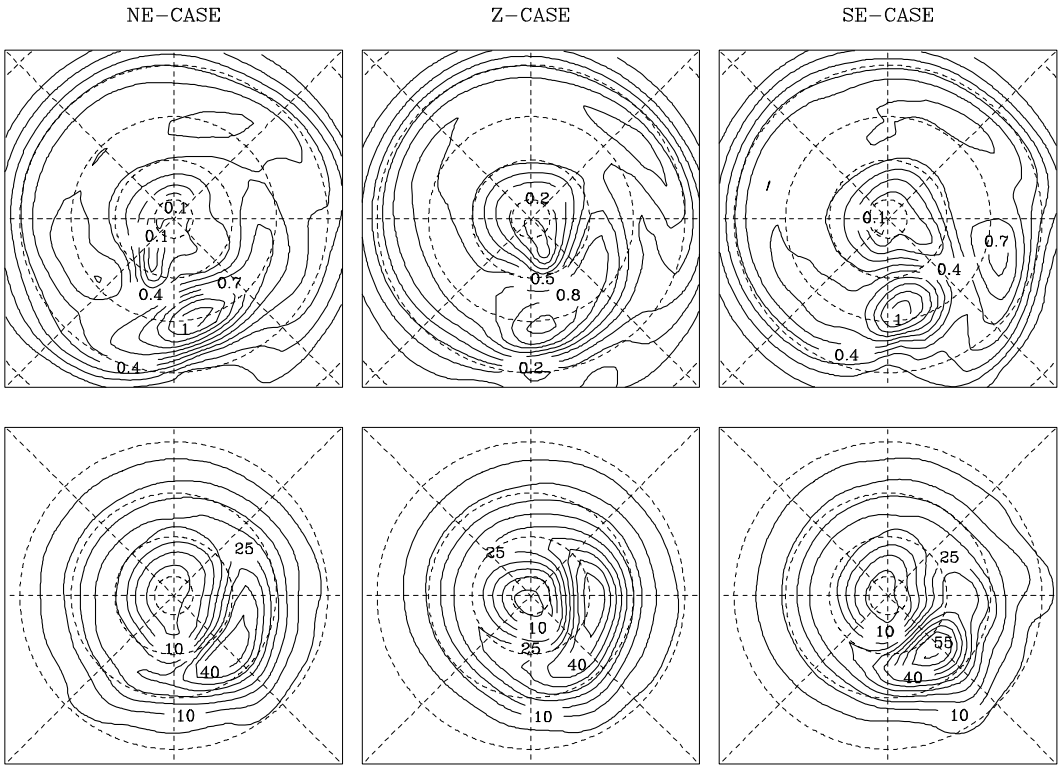

Figure 3: Maximum Eady growth rate (in 1/day, upper panels) and standard deviation of the band-pass filtered 500 hPa geopotential height (in gpm, lower panels), simulated in the NE-case (right column), in the Z-case (middle column) and in the SE-case (right column).

In the vertical, the amplitude of the temperature anomalies decreases to zero.

(ii) The interaction of two storm tracks

A second temperature dipole similar to the first one into the T_R field (Fig. 1b) is introduced. Only the NE-case is considered here. In a set of simulations the distance between the two dipoles changes from 180° to 130°.

(iii) The sensitivity of a storm track to large scale thermal forcing

Adding a temperature mono-pole on the warm pole side of the NE-case in the single storm track setup defines the third set of experiments (Fig. 1c). The zonal position of the mono-pole is the same as for the warm pole of the dipole. The sensitivity to mid-latitude large scale thermal forcing not unlike sea surface temperature anomalies in the real atmosphere is studied by varying the meridional position of this mono-pole (relative to the dipole).

4 Results

In all experiments, the introduction of zonal asymmetries into the forcing has only minor effects on the time mean zonally averaged circulation. However, the zonal asymmetric component of the flow is substantially modified in both, its time average and its variability.

(i) Organisation and variability of a single storm track

The sensitivity of the mean climate (i.e. the temporal average over the total simulation time excluding the spin-up) to the orientation of the heating dipole is illustrated in Figure 2 for selected fields. In all cases, the temperature distribution at 900 hPa (Fig. 2, upper panels) is controlled by the zonal asymmetries of the forcing. However the difference between the cold and the warm anomalies is reduced by approximately 50 % compared with the T_R field. A stationary high pressure center is located close to the cold anomaly in all simulations (Fig. 2, middle panels). In the NE- and Z-case, a stationary low emerges downstream at higher latitudes similar to the observed continental high and oceanic low configuration in the Northern Hemisphere winter. In contrast, in the SE-case a low is found upstream of the cold anomaly. Stationary waves are present in all three cases, which is evident in the 300 hPa meridional wind (Fig. 2, lower panels). Cyclonic (anticyclonic) shear is detected near the cold (warm) low level temperature anomaly. Further downstream, the stationary wave is radiated towards the south-east.

In all three experiments the heating dipole leads to an organization of a localized storm track, the position of which corresponds to the area of largest baroclinicity. Figure 3 (upper panels) displays the maximum growth rate σ_{BI} of an Eady wave (EADY, 1949) at 700 hPa as a

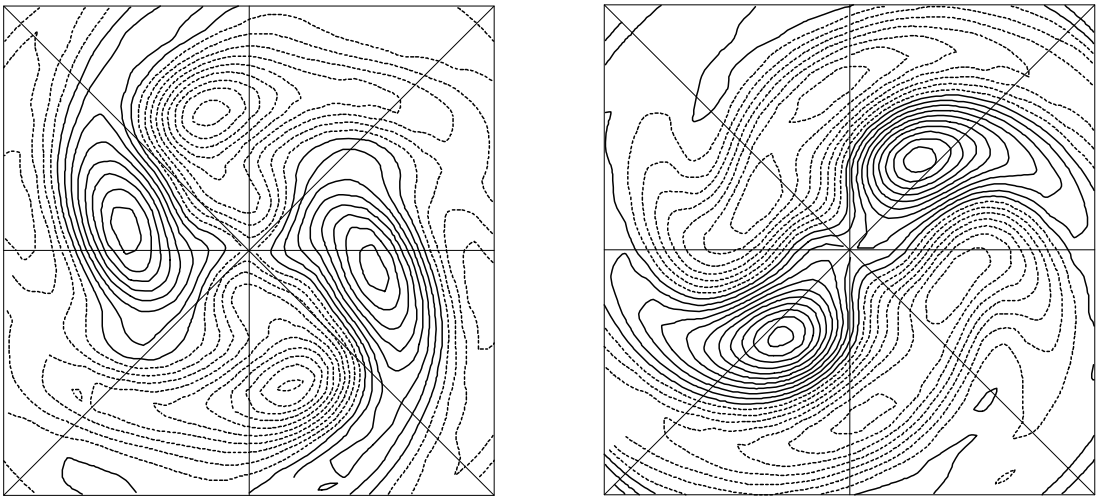

Figure 4: Real (left) and imaginary (right) part of the leading CEOF.

measure of baroclinicity, which is given by

$$\sigma_{BI} = 0.31 \frac{f}{N} \frac{\partial |v|}{\partial p} \qquad (4.1)$$

where f is the Coriolis parameter, N the Brunt Väisälä frequency, v the horizontal wind and p the pressure.

The storm track maximum measured by the band-pass filtered (TRENBERTH, 1991) 500 hPa geopotential-height temporal standard deviation is located downstream and northward of the σ_{BI} maximum (Fig. 3, lower panels). Compared to the SE-case, the storm track extends further downstream in the NE- and the Z-case. The position of the maximum standard deviation depends on the dipole orientation and is farthest downstream in the Z-case and closest to the dipole in the SE-case. Due to the coarse resolution and the lack of latent heat release the magnitude of the standard deviation amounts to 3/4 of observed values only.

Summarizing the results for the mean circulation and the transients, the NE-case is most similar to the observations. In this experiment, low-frequency variability can be detected which is associated with a retrograde propagating large scale wave pattern. However, since this feature is even more dominant in the experiments with two storm tracks, the discussion of the underlying mechanism is postponed to (ii).

(ii) Interaction of two storm tracks

First, the experiment with a zonal distance of 180° between the two heating dipoles is discussed. In this case two storm tracks emerge with climatologies of the zonally averaged flow and the stationary waves similar to those discussed in (i). The most prominent feature of this run is the occurrence of low-frequency variability already present in the one dipole run, but more regular and with larger amplitudes. An analysis employing a decomposition of the vertical averaged streamfunction into

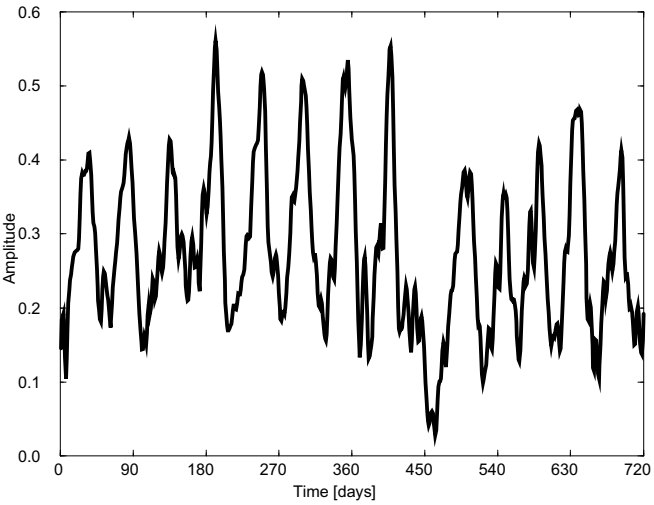

Figure 5: Amplitude time series of the leading CEOF.

complex empirical orthogonal functions (CEOFs) point out a wavenumber two retrograde travelling wave, which exhibits an amplitude modulation with a time scale of about 50 days. The leading CEOF explains 23 % of the total variance of the unfiltered (daily) data. The real (Re) and the imaginary (Im) part of this CEOF are displayed in Figure 4. Following the definition of CEOF the patterns evolve in the following sequence:

$$\ldots => \mathrm{Re} => \mathrm{Im} => -\mathrm{Re} => -\mathrm{Im} => \mathrm{Re} => \ldots$$

The imaginary part is associated with two large scale anticyclonic perturbations downstream of the jets hinting to a blocking-like event. These anticyclonic anomalies are followed downstream by cyclonic areas with weaker amplitudes. They are more zonally elongated than the anticyclones. The real part is shifted eastward with respect to the imaginary part. Exploring the amplitude time series of this CEOF (Fig. 5) a distinct modulation with a time scale of about 50 days is visible.

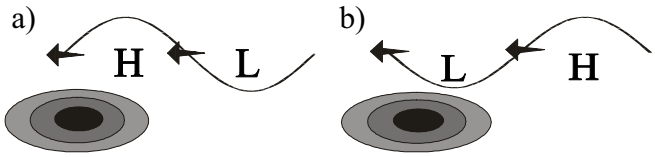

Figure 6: Sketch of the spatial resonance mechanism. The wave pattern represents the large scale eastward (arrows) propagating anomaly. The forcing by the storm track eddies is indicated by the shaded ellipses. The ridge (H) is amplified by passing the area of maximum eddy forcing (panel a) while the trough gets diminished at this location (panel b).

Also both, real and imaginary, parts of the corresponding complex principal component show an oscillation of 50 days. That is, the wave consists of a traveling part with a period of 50 days and an amplitude modulation of the same period. The evaluation of the phase indicate the retrograde propagation.

Spatial resonance: To identify the mechanism of amplitude modulation, an analysis of the streamfunction tendency equation for the low frequency flow is performed (CAI and VAN DEN DOOL, 1994; FELDSTEIN, 1998) by separating the stream function forcing into individual contributions of low-frequency and high-frequency variations. A cross spectrum analysis reveals that the self interaction of the high-frequency eddies and its time mean part force the amplitude modulation. Also, the interaction between the low- and high-frequency transients, the sum of tilting term and vertical vorticity advection and their respective time means act as a forcing. The phase relation shows that the initial forcing comes from the self-interaction of the high-frequencies leading the amplitude by 60°. Friction and the self-interaction of the low-frequencies damp the anomalies. Linear terms related to Rossby-wave motion drive the propagation of the anomalies. Figure 6 sketches the detected mechanism for the amplitude modulation which can be denoted as 'spatial resonance'.

Storm track separation: The sensitivity of the results to the prescribed distance of the forcing dipoles is investigated, because the distance between the two observed Northern Hemisphere storm tracks differs from the 180°. A set of experiments is performed with different distances ranging from 180° to 130°. The low-frequency variability in connection with a retrograde travelling wave is common for all experiments. However, a decreasing distance between the storm tracks is related to a broadening of the spectral 50 day maximum. It nearly vanishes in the experiment with the smallest distance (130°). In addition, the horizontal structure of the wave changes from wavenumber two to wavenumber one. The following analysis concentrates on the 150° case which approximately corresponds to the observed distance between Pacific and Atlantic storm track. Figure 7 compares the 180° and the 150° climatologies by means of the standard deviation of the (3 to 6 day) bandpass filtered 500 hPa geopotential height as a measure for the storm track intensity. While in the 180° case two identical storm tracks emerge, intensity and extension varies in the 150° run. The area with a smaller distance (referred to as P-Area, according to 'Pazific' area) exhibits a stronger storm track than the other area (referred to as A-Area, according to 'Atlantic' area). Also, the strength of the P-area storm track exceeds the strength of the storm tracks in the 180° experiment, whereas the A-area storm track is weaker than the 180° reference.

Teleconnections: Low-frequency variability connecting remote locations is characterized by teleconnection patterns deduced from the correlation matrix (WALLACE and GUTZLER, 1981). Teleconnection patterns based on monthly means of the 300 hPa streamfunction for the 180° and the 150° simulation are shown in Figure 8 together with local correlation maps for points of maximum teleconnectivity. In the 180° experiment, the patterns are similar to the retrograde travelling wave pattern discussed above. In the 150° experiment the P-area is dominated by a quadrupole (P-pattern) centered in the storm track which originates in the subtropics. In the A-area a dipole structure describing a meridional sea-saw (A-pattern) emerges. P-Pattern and A-pattern are remarkable similar to the observed Pacific North American (PNA) pattern and the North Atlantic Oscillation (NAO).

Life cycle: The life cycle of the P-pattern and the A-pattern is investigated using daily averages of the vertical mean streamfunction anomalies. Composite analysis and decomposition of the barotropic streamfunction tendency are used to identify the spatial-temporal behavior and the underlying mechanisms. Figure 9 and Figure 10 display the composite life cycles for the A- and P-pattern, respectively, for positive anomalies (negative cases are similar but of opposite sign). The A-pattern dynamics is associated with a retrograde travelling large scale Rossby wave. It originates in the center of the A-area storm track about 20 days before the anomalies reach their maximum (zero lag). The wave amplifies when the high pressure area passes the storm track region and decays afterwards. The streamfunction tendencies indicate that the mechanism of the wave amplification is the spatial resonance mechanism discussed in the 180° experiment (see above). A positive P-pattern anomaly is associated with a positive large scale anomaly which is stationary during the life cycle. It amplifies until zero lag and decays thereafter with an upstream development, indicating a wave dispersion which resembles the life cycle of a persistent blocking event. Here, the barotropic streamfunction tendencies do not indicate any significant contribution to the amplification. This hints to baroclinic processes governing the P-pattern life cycle.

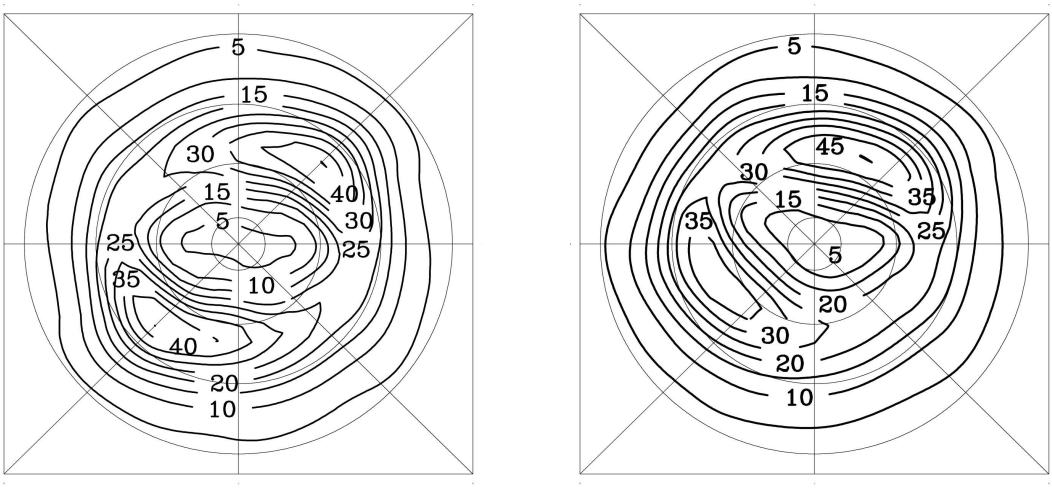

Figure 7: Standard deviation of the band-pass filtered 500 hPa geopotential height (in gpm) for the 180° case (left) and the 150° case (right).

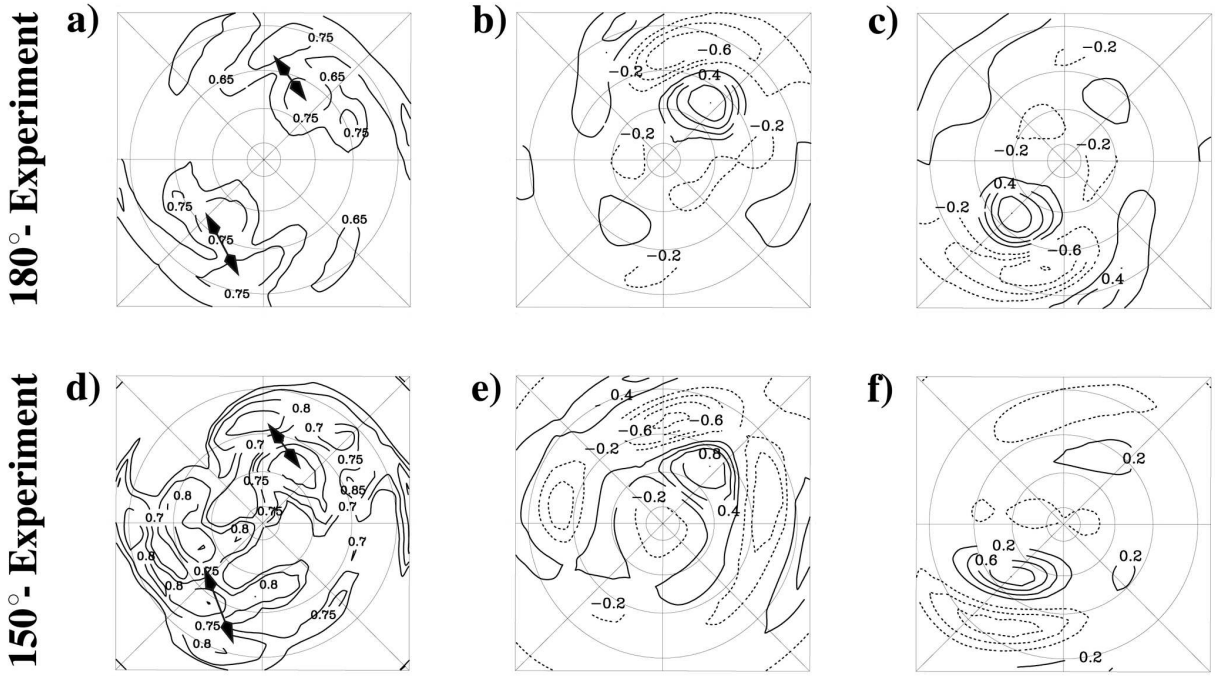

Figure 8: Teleconnectivity (panels a and d) and point correlation maps (panels b, c, e, f) of the 300 hPa geopotential height for the 180° case (panels a–c) and the 150° case (panels d–f). Point correlations are computed using base points at the arrowheads displayed in panel a and panel d.

(iii) Sensitivity to large scale thermal forcing

A non-linear response of storm tracks, stationary waves and low frequency variability arises by adding a thermal forcing monopole to the NE-dipole. A positive T_R anomaly in the warm center of the dipole leads to a poleward shift of the eddy activity. A poleward shift of the monopole weakens the storm track while an equatorward shift enforces the eddies. In contrast, a cold anomaly in the warm center diminishes the synoptic activity. Here, a poleward shift reinforces the storm track and an equatorward shift attenuates the eddy activity.

Figure 11 displays the response of the band-pass filtered 500 hPa geopotential height standard deviation to a warm and to a cold monopole anomaly of 25 K magnitude centered in the warm pole of the NE-dipole.

The stationary response consists of a baroclinic and an equivalent barotropic component. The baroclinic component is located near the warm (cold) monopole with a lower level trough (ridge) and an upper level ridge (trough). The equivalent barotropic response appears further downstream with maximum amplitude in the upper troposphere. Positive (negative) anomalies of the geopotential show up for a warm (cold) monopole.

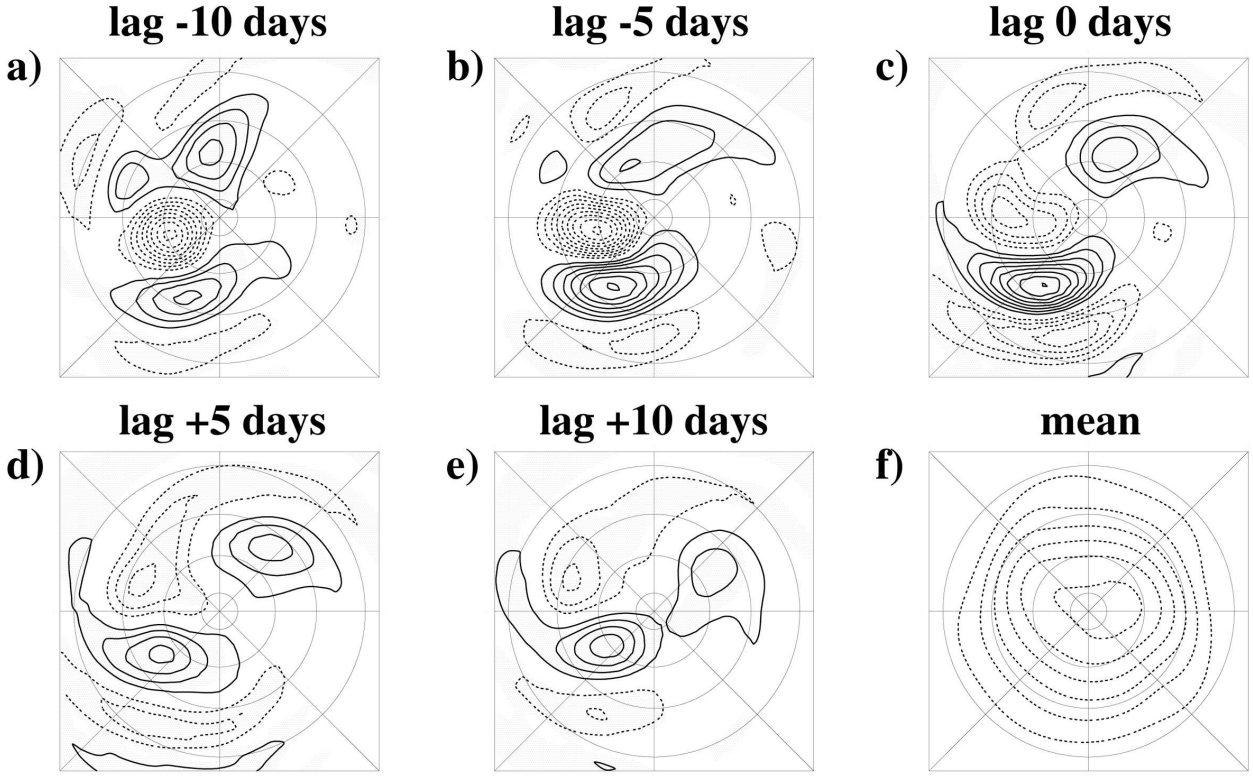

Figure 9: Composite life cycle of the A-pattern (vertical averaged stream function) for positive anomalies for different time lags: (a) –10 days, (b) –5 days, (c) 0 days, (d) +5 days, (e) +10 days (contour interval is $5x10^5$ m^2s^{-1}). (f) shows the time average (contour interval is 10^7 m^2s^{-1}).

Eddy feedback has little impact on the baroclinic component. However, the equivalent barotropic part is significantly enhanced, if the pattern is in phase with the streamfunction forcing by the synoptic eddies as it is the case for the warm monopole only.

The low frequency variability is also affected by the monopole forcing. In the warm monopole case the variance of the retrograde travelling large scale Rossby wave which is observed in the storm track only case (see above) is increased. Standing wave components contribute more to the low frequency variability and, partially, blocking-like events develop. Two different teleconnection patterns (not shown) can be identified which are related to wave trains induced by the warm monopole and the dipole, respectively.

5 Discussion and conclusions

The simplified atmospheric global circulation model PUMA is used to investigate physical mechanisms leading to the observed circulation patterns and their variability: (i) The organization and variability of a localized singe storm track, (ii) the interaction of two storm tracks and the induced low frequency variability and (iii) the response of a storm track to large scale thermal forcing. The results highlight the role and the importance of the storm track dynamics for the mean circulation, its low-frequency variability and its response to external forcing.

(i) Organisation and variability of a single storm track

A localized storm track is established by a zonally asymmetric distribution consisting of a heating dipole embedded in a zonally symmetric profile. The orientation of the dipole affects the characteristics of the storm track and the background flow. The NE-case, a north-east orientation of the dipole, shows the most realistic climatology. The mean circulation and the distribution of the transient eddies are in good agreement with observations of the Northern Hemisphere winter (BLACKMON et al., 1977). Local baroclinic instability appears to be responsible for the localization of eddy kinetic energy. The zonal variation of baroclinicity is mainly maintained by the heating, consistent with the results of HOSKINS and VALDES (1990).

(ii) Interaction of two storm tracks

Low-frequency variability already present in the singe storm track NE-case experiment becomes more evident

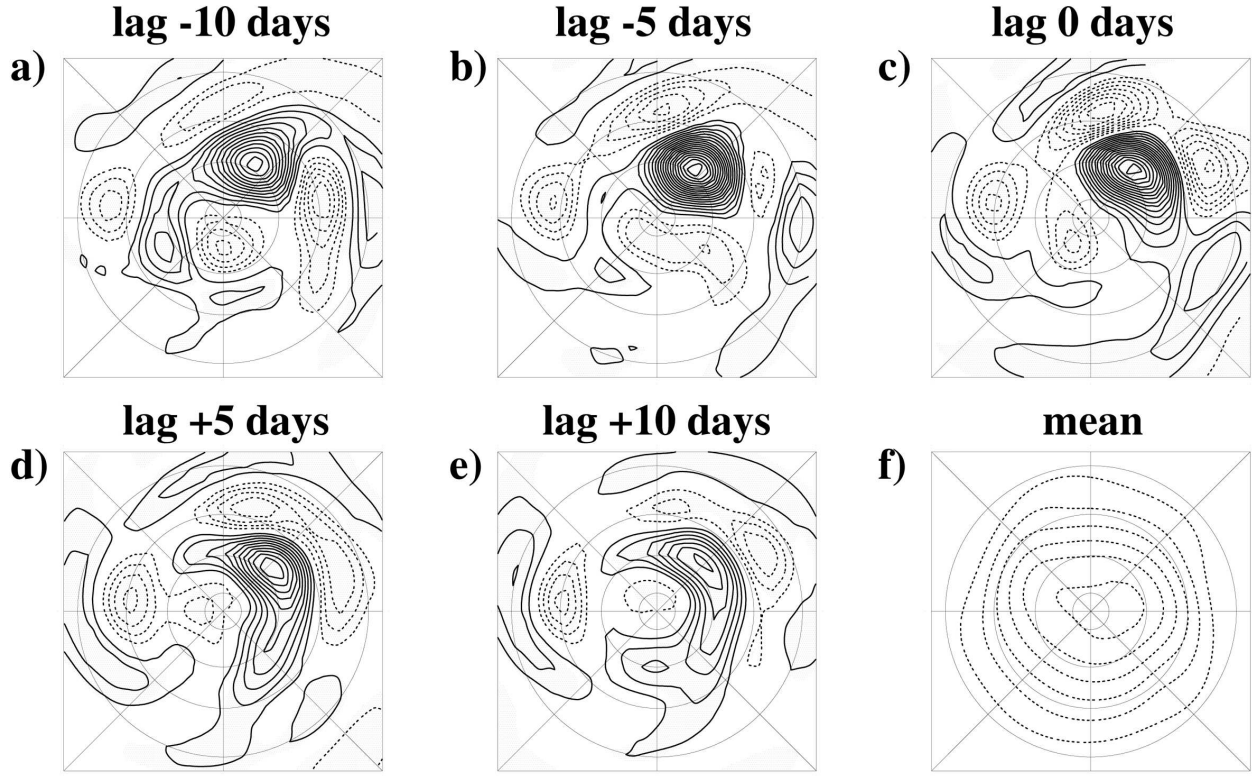

Figure 10: Composite life cycle of the P-pattern (vertical averaged stream function) for positive anomalies for different time lags: (a) –10 days, (b) –5 days, (c) 0 days, (d) +5 days, (e) +10 days (contour interval is $5x10^5$ m^2s^{-1}). (f) shows the time average (contour interval is 10^7 m^2s^{-1}).

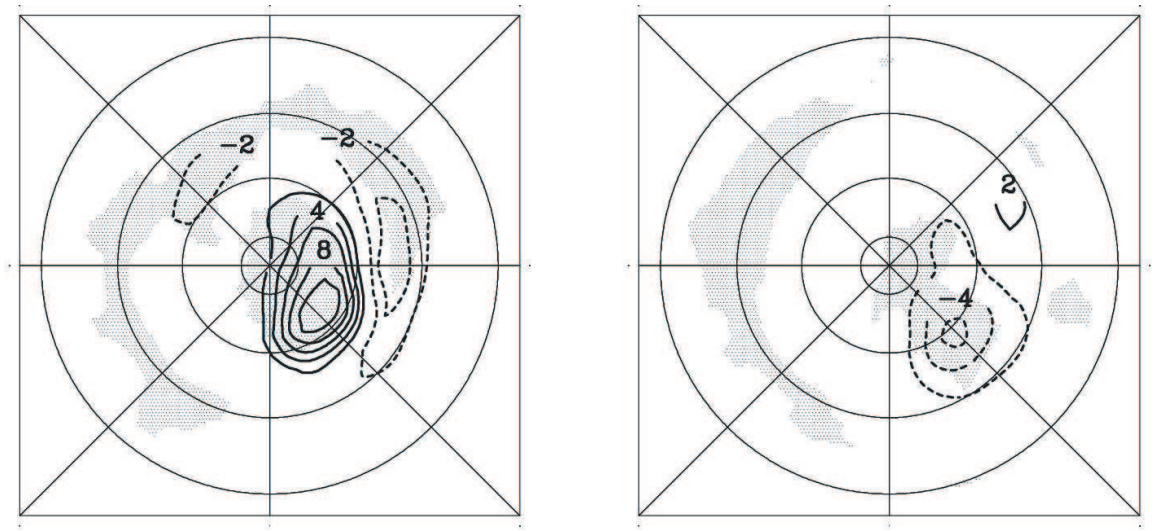

Figure 11: Response of the standard deviation of the band-pass filtered 500 hpa geopotential height (in gpm) for a warm (left) and a cold (right) anomaly of 25 K centered in the warm pole of the forcing dipole.

if a second storm track is included. However, The characteristics and the underlying mechanisms of the variability proof to be sensitive to the distance of the two storm tracks. In the 180° case a retrograde travelling large scale Rossby wave with an amplitude modulation of nearly 50 days dominates the variability. In observations retrograde travelling wave are identified by KUSHNIR (1987); LANZANTE (1990); LAU and NATH (1999) and BRANSTATOR (1987). In contrast to KUSHNIR the variability in the model is related to a blocking anti-cyclone at the end of the storm track while KUSHNIR found a random distribution of the anomalies. In the model, the amplitude modulation is cased by a spatial resonance between the low-frequency wave and the

forcing by high-frequency storm track eddies. A similar mechanism can be found in a shallow water ocean model (SURA et al., 2000). The pattern of the variability is in a general correspondence with the so-called P3-Mode for the Pacific (LAU, 1988). The connection between the blocking anti-cyclone and the synoptic eddies agrees with blocking case studies (COLUCCI, 1985) and with studies concerning the maintenance of blockings by synoptic eddies (MULLEN, 1987). A hydrodynamic instability causing the low-frequency variations as proposed by FREDERIKSEN (1982); SIMMONS et al. (1983) or KUSHNIR (1987) is not supported by the model.

In the 150° case two different patterns of low-frequency variability arise, which are in remarkable agreement with the observed North Atlantic Oscillation and Pacific North American teleconnection patterns introduced by (WALLACE and GUTZLER, 1981). Life cycles of both teleconection patterns (A-pattern and P-pattern) are investigated. The time scale for both teleconnetions is about 50 days. While the spatial resonance mechanism, already identified in the 180° case, is responsible for the A-pattern life cycle, baroclinic processes affect the P-pattern variability consistent with the results of BLACK (1997) and BLACK and DOLE (1993), who investigated the development of persistent anomalies in the North Pacific area.

(iii) Sensitivity to large scale thermal forcing: The response of the single storm track circulation to large scale thermal forcing demonstrates the importance of the eddies. A non-linear response is observed depending on the sign and the position of the additional forcing. A baroclinic and an equivalent barotropic signal is observed. Qualitatively, the results are in good agreement with other modeling studies (PALMER and SUN, 1985; PITCHER et al., 1985; LAU and NATH, 1990). In particular, the non-linearity is supported by other investigations (PITCHER et al., 1988; ROBERTSON et al., 2000). The effect of the storm track eddies on the strength of the equivalent barotropic part, as it shows up in the sensitivity experiments, may account for different results obtained by coarse and high resolution general circulation models (FRANKIGNOUL, 1985; PENG et al., 1997) since the representation of synoptic eddies varies substantially with resolution.

In summary, the results presented in this paper show the ability of gaining insight into physical mechanisms affecting the atmospheric circulation and its variability by using simplified models. The studies focus on the effect of a localized storm tracks as a dominant feature of the Northern Hemisphere circulation. The results indicate the importance of the storm track eddies and their feedbacks for the characteristics of the observed variability like teleconnection patterns. However, the studies presented here show the effect of thermal forcing in organizing the storm tracks or exiting large scale circulation anomalies. It is apparent that for the Northern Hemisphere circulation the influence of orography may also be important. Therefore, the role of orographically forced stationary waves and the interaction of these waves with the circulation (in particular with the storm tracks) will be the focus of future studies.

Acknowledgements

This paper comprises SFB-related research on storm tracks and low frequency variability based on experiments with a simple GCM under idealized conditions. While most details (and figures) are published, this summarizing view has been prepared under the SFB-leitmotif and connection with the other research projects. Klaus DETHLOFF's and another referee's comments are greatfully acknowledged.

References

BJERKNES, J., 1964: Atlantic air-sea interaction. – Adv. in Geophys. **10**, 1–82.

BLACK, R.X., 1997: Deducing anomalous wave source regions during the life cycles of persistent flow anomalies. – J. Atmos. Sci. **54**, 895–907.

BLACK, R.X., R.M. DOLE, 1993: The Dynamics of Large-Scale Cyclogenesis over North Pacific Ocean. – J. Atmos. Sci. **50**, 421–442

BLACKMON, M.L., 1976: A climatological spectral study of the 500mb geopotential height of the northern hemisphere. – J. Atmos. Sci. **33**, 1607–1623.

BLACKMON, M.L., J.M. WALLACE, N.-C. LAU, S.L. MULLEN, 1977: An observational study of the northern hemisphere wintertime circulation. – J. Atmos. Sci. **34**, 1040–1053.

BRANSTATOR, G., 1987: A striking example of the atmospheres's leading traveling pattern. – J. Atmos. Sci. **44**, 2310–2323.

CAI, M., H.M. VAN DEN DOOL, 1994: Dynamical decomposition of low-frequency tendencies. – J. Atmos. Sci. **51**, 2086–2100.

CHANG, E.K., I. ORLANSKI, 1993: On the dynamiks of a storm track. – J. Atmos. Sci. **50**, 999–1015.

COLUCCI, S.J., 1985: Explosive cyclogenesis and large-scale circulation changes: Implications for atmospheric blocking. – J. Atmos. Sci. **42**, 2701–2717.

EADY, E.T., 1949: Long waves and cyclone waves. – Tellus **1**, 33–52.

ELIASEN, E., B. MACHENHAUER, E. RASMUSSEN, 1970: On the numerical method for integration of the hydrodynamical equations with a spectral representation of the horizontal fields. – Inst. of Theor. Met. Univ. of Copenhagen, No. **2**.

FELDSTEIN, S.B., 1998: The growth and decay of low-frequency anomalies in a GCM. – J. Atmos. Sci. **55**, 415–428.

—, 2002: Fundamental mechanisms of PNA teleconnection pattern growth and decay. – Quart. J. Roy. Meteor. Soc. **128**, 775–796.

FRAEDRICH, K., C. BANTZER, U. BURKHARDT, 1993: Winter climate anomalies in Europe and their associated circulation at 500 hPa. – Climate Dyn. **8**, 161–175.

FRAEDRICH, K., E. KIRK, F. LUNKEIT, 1998: PUMA: Portable University Model of the Atmosphere. – Deutsches Klimarechenzentrum, Technical Report **16**, 38 pp.

FRANKIGNOUL, C., 1985: Sea surface temperature anomalies, planetary waves and air-sea feedback in the middle latitudes. – Rev. Geophys. **23**, 357–390.

FRANZKE, C., K. FRAEDRICH, F. LUNKEIT, 2000: Low frequency variability in a simplified atmospheric GCM: Storm track induced spatial resonance. – Quart. J. Roy. Meteor. Soc. **126**, 2691–2708.

—, —, —, 2001: Teleconnections and low-frequency variability in idealised experiments with two storm tracks. – Quart. J. Roy. Meteor. Soc. **127**, 1321–1339.

FREDERIKSEN, J.S., 1982: A unified three-dimensional instability theory of the ondet of blocking and cyclogenesis. – J. Atmos. Sci. **39**, 969–982.

FRISIUS, T., F. LUNKEIT, K. FRAEDRICH, I.N. JAMES, 1998: Storm-track organisation and variability in a simplified atmospheric global circulation model. – Quart. J. Roy. Meteor. Soc. **124**, 1019–1043.

HELD, I.M., 1983: Stationary and quasi-stationary eddies in the extratropical troposphere: Theory. – In: HOSKINS R.P., PEARCE, R.P. (Eds): Large-scale dynamical processes in the atmosphere, Academic Press, 127–168.

HELD, I.M., M.J. SUAREZ, 1994: A proposal for the intercomparison of the dynamical cores of atmospheric general circulation models. – Bull. Amer. Meteor. Soc. **75**, 1825–1830.

HOSKINS, B.J., A.J. SIMMONS, 1975: A multi-layer spectral model and the semi-implicit method. – Quart. J. Roy. Meteor. Soc. **101**, 637–655.

HOSKINS, B.J., P.J. VALDES, 1990: On the existence of storm-tracks. – J. Atmos. Sci. **47**, 1854–1864.

JAMES, I.N., L.J. GRAY, 1986: Concerning the effect of surface drag on the circulation of a planetary atmosphere. – Quart. J. Roy. Meteor. Soc. **112**, 1231–1250.

KUSHNIR, Y. 1987: Retrograding wintertime low-frequency disturbances over the North Pacifik ocean. – J. Atmos. Sci. **44**, 2727–2742.

LANZANTE, J.R. 1990: The leading modes of 10–30 day variability in the extratropics of the northern hemisphere during the cold season. – J. Atmos. Sci. **47**, 2115–2140.

LAU, N.-C., 1979a: The structure and energetics of transient disturbances in the northern hemisphere wintertime circulation. – J. Atmos. Sci. **36**, 982–995.

—, 1988: Variability of the observed midlatitude storm tracks in relation to low-frequency changes in the circulation pattern. – J. Atmos. Sci. **45**, 2718–2743.

—, 1979b: The observed structure of tropospheric stationary waves and the local balance of vorticity and heat. – J. Atmos. Sci. **36**, 996–1016.

—, 1997: Interactions between global SST anomalies and the midlatitude atmospheric circulation. – Bull. Amer. Meteor. Soc. **78**, 21–33.

LAU, N.-C., M.J. NATH, 1990: A general circulation model study of the atmospheric response to extratropical SST anomalies observed in 1959–1979. – J. Climate **3**, 965–989.

—, —, 1999: Observed and GCM-simulated westward-propagating, planetary-scale fluctuations with approximately three-week periods. – Mon. Wea. Rev. **127**, 2324–2345.

MULLEN, S.L., 1987: Transient eddy forcing of blocking flows. – J. Atmos. Sci. **44**, 3–22.

ORSZAG, S.A., 1970: Transform method for calculation of vector coupled sums. – J. Atmos. Sci. **27**, 890–895.

PALMER, T.N., Z. SUN, 1985: A modelling and observational study of the relationship between sea surface temperature in the North-West Atlantic and the atmosphere general circulation. – Quart. J. Roy. Meteor. Soc. **111**, 947–975.

PENG, S., W.A. ROBERTSON, M.P. HOERLING, 1997: The modeled atmospheric response to midlatitude SST anomalies and its dependence on background circulation states. – J. Climate **10**, 971–987.

PITCHER, E.J., M.L. BLACKMON, G.T. BATES, S. MUNOS, 1988: The effect of North Pacific sea surface temperature anomalies on the January climate of a general circulation model. – J. Atmos. Sci. **45**, 173–188.

ROBERTSON, A.W., C.R. MECHOSO, Y.-J. KIM, 2000: The influence of Atlantic sea surface temperature anomalies on the North Atlantic Oscillation. – J. Climate **13**, 122–138.

SICKMÖLLER, M., R. BLENDER, K. FRAEDRICH, 2000: Observed winter cyclone tracks on the northern hemisphere in re-analysed ECMWF data. – Quart. J. Roy. Meteor. Soc. **126**, 591–620.

SIMMONS, A.J., J.M. WALLACE, G.W. BRANSTATOR, 1983: Barotropic wave propagation and instability, and atmospheric teleconnection patterns. – J. Atmos. Sci. **40**, 1363–1392.

SMAGORINSKY, J., 1953: The dynamical influence of large-scale heat sources and sinks on the quasi-stationary mean motion of the atmosphere. – Quart. J. Roy. Meteor. Soc. **79**, 342–366.

SURA, P., F. LUNKEIT, K. FRAEDRICH, 2000: Decadal variability in a simplified wind-driven ocean model. – J. Phys. Oceanogr. **30**, 1917–1930.

TING, M., 1994: Maintenance of northern summer stationary waves in a GCM. – J. Atmos. Sci. **51**, 3286–3308.

TRENBERTH, K.E., 1991: Storm tracks in the southern hemisphere. – J. Atmos. Sci. **48**, 2159–2178.

WALLACE, J.M., D.S. GUTZLER, 1981: Teleconnections in the geopotential height field during northern hemisphere winter. – Mon. Wea. Rev. **109**, 784–812.

WALTER, K., U. LUKSCH, K. FRAEDRICH, 2001: A response climatology of idealized midlatitude thermal forcing experiments with and without a storm track. – J. Climate **14**, 467–484.